REVIEWS OF TOPICAL PROBLEMS

Tunneling and barrier-suppression ionization of atoms and ions in a laser radiation field

Physics – Uspekhi **41** (5) 469 – 485 (1998)

REVIEWS OF TOPICAL PROBLEMS PACS numbers: **32.90.+a**, **42.65.+k**

Tunneling and barrier-suppression ionization of atoms and ions in a laser radiation field

N B Delone, V P Krainov

Contents

Abstract. Experimental and theoretical data on tunneling and barrier-suppression ionization of atoms and atomic ions in a low-frequency laser radiation field are considered. The yields of single- and multi-charged ions, the energy and angular distributions of photoelectrons, and effects of the laser pulse length and laser polarization are analyzed.

1. Introduction

Immediately after the discovery of lasers at the beginning of the sixties, both experimenters and theoreticians became interested in the process of nonlinear ionization of atoms and ions. This is the main process in the interaction of powerful laser radiation with matter. Its investigation was based on known laws for the ionization of atomic particles with a constant electric field (the tunneling effect and above-barrier decay) and for single-photon ionization. It was clear that in the nonlinear case when the photon energy is less than the atomic ionization potential, analogous nonlinear processes should also occur. Such processes are multiphoton ionization, the tunneling effect and above-barrier decay in a variable field. A theoretical description of these processes and an experimental verification of theoretical results should be developed. First of all, it was important to find interrelation between the above processes.

Among the many papers we should like to underline the work of L V Keldysh [1]. Its results are fundamental for the modern theory of nonlinear ionization by a variable field with a field strength which is small compared to the atomic field strength. Two principal results were obtained in this work using a model of the short-range atomic potential.

Firstly, it was found that multiphoton and tunneling ionization are two limiting cases of the universal process of nonlinear ionization; this process is determined by three parameters — the laser frequency ω, the amplitude of the laser field strength F, and the atomic ionization potential E_i.

In the *multiphoton* limit the ionization rate depends on the field strength according to the power law:

$$w \propto F^{2K},$$

where $K = \langle E_i/\omega + 1 \rangle$ is the number of absorbed photons; here $\langle \ldots \rangle$ means the integral part of this number. (We use the atomic system of units $e = m_e = \hbar = 1$.)

In the *tunneling* limit the ionization rate increases exponentially with the field strength; it is of a simple form (with exponential accuracy):

$$w \propto \exp\left[-\frac{2(2E_i)^{3/2}}{3F}\right]. \qquad (1)$$

N B Delone General Physics Institute, Russian Academy of Sciences, ul. Vavilova 38, 117942 Moscow, Russia
Tel. (7-095) 135-02 96
V P Krainov Moscow Institute of Physics and Technology, 141700 Dolgoprudny, Moscow Region, Russia
E-mail: krainov@theory.mipt.ru

Received 25 November 1997
Uspekhi Fizicheskikh Nauk **168** (5) 531 – 549 (1998)
Translated by V P Krainov; edited by L V Semenova

For example, the tunneling ionization rate for the ground state of a hydrogen atom by a circularly polarized electromagnetic field is given by the well-known expression (at $F \ll 1$):

$$w = \frac{4}{F}\exp\left(-\frac{2}{3F}\right). \tag{2}$$

In the case of a linearly polarized field we should substitute $F \to F\cos\omega t$ in Eqn (2) and average the ionization rate over the field period. Then we obtain an expression which differs from Eqn (2) by pre-exponential factor only:

$$w = 4\sqrt{\frac{3}{\pi F}}\exp\left(-\frac{2}{3F}\right). \tag{3}$$

Secondly, it was shown that the boundary between multiphoton and tunneling ionization is determined by the value of the so called *adiabaticity parameter*:

$$\gamma = \frac{\omega\sqrt{2E_i}}{F}. \tag{4}$$

The values of $\gamma^2 \gg 1$ correspond to *multiphoton* ionization; this process is realized at a relatively high frequency and low field strength of laser radiation. Oppositely, the values of $\gamma^2 \ll 1$ correspond to *tunneling* ionization, which is realized at a low frequency and high field strength. Thus, at a fixed radiation frequency first multiphoton ionization and then tunneling ionization should take place. This is shown schematically in Fig. 1.

Besides the different dependence of the ionization rate on the field strength F, both processes have different dependences on the radiation frequency ω. The rate for multiphoton ionization of an atom or of an ion depends sharply on the radiation frequency due to intermediate (including multiphoton) resonances between the energy of some number of absorbed photons $N < K$ and the transition energy in the discrete atomic spectrum. An interesting experiment [2] demonstrates the transition from the multiphoton to the tunneling ionization at a fixed radiation frequency for the increasing field intensity. In Figure 2 the electron energy spectrum is depicted. For the tunneling ionization (Fig. 2b) it does not contain narrow peaks which occur in the above-threshold multiphoton ionization. These peaks are explained by the absorption of an excess number of photons compared to the minimum number permitted by the energy conservation law, and also by resonances with the intermediate discrete atomic levels (Fig. 2a).

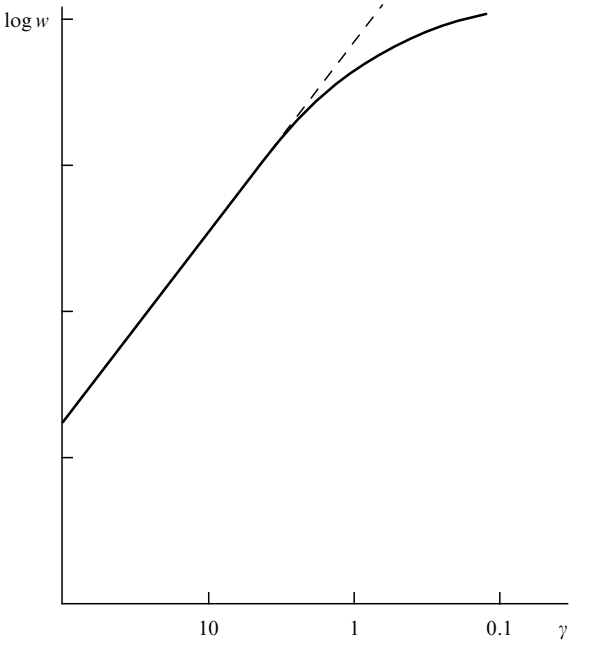

Figure 1. Schematic dependence of the logarithm of the ionization probability on the adiabaticity parameter γ.

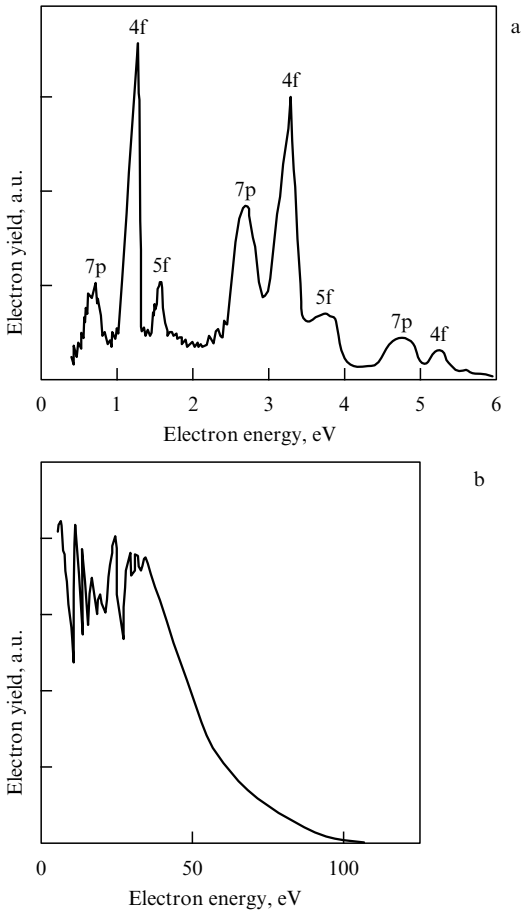

Figure 2. Electron energy spectrum in the ionization of atoms: (a) Xe ($\gamma = 2 - 8$); (b) He ($\gamma = 0.5 - 1$) [2].

2. Tunneling and barrier-suppression ionization

Numerous investigations made after the above cited work [1] have given today's detailed picture of the process of multiphoton ionization of atoms and atomic ions [3 – 5]. However, the tunneling effect and, especially, above-barrier decay have been less investigated. The reason is that for many years experimenters observed the tunneling effect only in a field of IR laser radiation (low radiation frequency ω). For example, the first convincing observations of tunneling ionization were obtained using IR radiation of a CO_2-laser with frequency $\omega \sim 0.1$ eV [6]. Recently progress in power lasers has allowed the observation of tunneling ionization and above-barrier

decay using high intense visible light. Therefore it is interesting to compare all the data on these processes obtained over recent years.

Investigations of above-barrier decay are still in the initial stages. The barrier-suppression field strength F_{BSI} is determined from the condition that the atomic ionization potential is equal to the top of the effective one-dimensional potential barrier in a constant electric field:

$$F_{\mathrm{BSI}} = \frac{E_{\mathrm{i}}^2}{4Z} . \tag{5}$$

Here Z is the charge of the atomic core. However, this formula does not take into account two important circumstances. Firstly, it follows from quantum mechanics that above-barrier reflection occurs; part of the electrons are reflected back from the top of the barrier. The probability of penetration achieves unity at the essential excess of energy above the top of the barrier only, i.e. at a value of the field strength which is greater than F_{BSI} from Eqn (5). Secondly, we should take into account the AC Stark shift in order to obtain the correct value of the barrier-suppression field strength. It was found that the correct value for the barrier-suppression field strength is greater than the estimate (5). Finally, the competition of tunneling ionization on the edge of laser pulse at $F < F_{\mathrm{BSI}}$ can be important for the significant durations of the laser pulses in experiments.

In comparing the experimental data with theoretical predictions some methodical factors should be taken into account. Any theoretical approach is applied to an isolated atom and to monochromatic radiation with a fixed field strength (fixed radiation intensity). Meanwhile, the total yield of ions (or of electrons) produced in the target (for example, in a rarified gas) by the laser radiation with a spatial-temporal distribution of intensity is measured in the experiments. The quantities which are proportional to the total ionization probability $W = w\tau$ (τ is the length of the laser pulse) are measured in the experiments; hence, ionization saturation can occur, when instead of above dependence we have $W \sim 1$. The inhomogeneous distribution of radiation in the target can mean that some lower value of the intensity is the most effective instead of the maximum intensity in the center of the spatial-temporal distribution. Besides this, most atoms may be ionized on the edge of the laser pulse. Then the ionization process at the maximum of intensity does not occur, in general.

Therefore at the all stages of experimental investigation of nonlinear ionization from the experimental project up to data processing we should take into account the possibility of saturation and of a spatial-temporal inhomogeneity of distribution.

Finally, the general situation for obtaining experimental data should be clearly explained. In theoretical derivations we can fix the laser frequency and vary the laser intensity; then we can obtain the excitation curve including all three regimes of ionization: multiphoton ionization, the tunneling effect and above-barrier decay. However, any experiment with a fixed atom and fixed parameters of the laser pulse gives only one point on this excitation curve. Because of the large nonlinearity of the ionization process the ionization rate for a lower radiation intensity is very small, so that the total number of ions (or electrons) will be less than the threshold of the experimental set; but at a greater radiation intensity the saturation occurs quickly. Therefore only the combination of results of many experiments with different atoms and ions having different ionization potentials, radiated by laser pulses with different frequencies and durations, can give a general picture of the process of nonlinear ionization. Even for observation of the narrow transition region between tunneling and multiphoton ionization several atomic substances are needed (see Fig. 2).

Finally, it should be noted that electron energy and angular distributions in the tunneling and barrier-suppression ionization give important information about the processes. However, experimental investigation of the electron spectra is difficult since these spectra are distorted on the way from the parent ion up to the detector due to the ponderomotive acceleration of electrons in the inhomogeneous field of laser radiation. Therefore, only for extremely small laser pulse lengths, these distortions are negligibly small, since an electron does not change its coordinates during the laser pulse. Another method can also be used; this is connected with taking into account the inhomogeneous field upon moving electrons. But this method is realized only using cumbersome computer calculations.

Below we consider experimental data and theoretical approaches to the tunneling effect and above-barrier decay of atoms in a variable field. Some of this material has been generalized previously in some reviews [7–10] and in a monograph [5]. Therefore the main attention will be devoted to the new data.

3. Rates for the tunneling ionization of atoms and ions by a laser radiation field

The rate of tunneling ionization for an excited state of a hydrogen atom with principal quantum number n, orbital quantum number l, and magnetic quantum number m by a *linearly* polarized field of laser radiation has been obtained in Ref. [11] (see also the monograph [5]):

$$w = \sqrt{\frac{3n^3F}{\pi}} \frac{(2l+1)(l+|m|)!2^{4n-2|m|-2}n^{-6n+3|m|}}{(n+l)!(n-l-1)!(|m|)!(l-|m|)!} \times \frac{\exp\left[-2/(3n^3F)\right]}{F^{2n-|m|-1}} . \tag{6}$$

This expression is applicable when the field strength is small compared to the atomic field strength (5), i.e. compared to the quantity $1/16n^4$. In the case of a circularly polarized field a relation analogous to Eqn (6) is valid, without the factor $\sqrt{3n^3F/\pi}$. In the case of the ground state of the hydrogen atom, Eqn (6) reduces to Eqn (3), as expected.

We consider further the case of complex atoms and atomic ions. Using the method of the quantum defect, we substitute the principal quantum number n by the effective principal quantum number

$$n^* \equiv \frac{Z}{\sqrt{2E_{\mathrm{i}}}} .$$

After such a substitution into Eqn (6) and using the Stirling formula for factorials we obtain in the case of a linearly polarized field (an s-state is taken for simplicity) [12]:

$$w_{\mathrm{ADK}} = \sqrt{\frac{3n^{*3}F}{\pi Z^3}} \frac{FD^2}{8\pi Z} \exp\left(-\frac{2Z^3}{3n^{*3}F}\right), \tag{7}$$

(this is so called ADK formula).

The notation introduced here will often be used below:

$$D \equiv \left(\frac{4eZ^3}{Fn^{*4}}\right)^{n^*}. \tag{8}$$

In the case of a circularly polarized field the ionization rate is of a more simple form:

$$w_{\mathrm{ADK}} = \frac{FD^2}{8\pi Z}\exp\left(-\frac{2Z^3}{3n^{*3}F}\right). \tag{9}$$

It is seen from Eqn (6) that the ionization rate for states with a nonzero magnetic quantum number is small compared to the ionization rate for the state with zero magnetic quantum number (for the same values of other parameters). The corresponding expressions can be found in Ref. [12]. It should be noted that in the averaging over the magnetic quantum numbers of the binding state being considered (this takes place in the case of identical populations of these states) the result for the ionization rate coincides with Eqns (7), (9). Thus, these expressions can be used practically for all atoms and positive ions with arbitrary charge multiplicity.

Of course, the application of the Stirling formula is formally only correct for large values of the principal quantum numbers. However, it is valid with a good accuracy even for ground states of atomic systems for numerical reasons [12].

Let us consider the applicability of the expressions obtained. The Stark decrease of the atomic ground levels diminishes the ionization rate. In principle, if the AC Stark shift is known, we can simply modify Eqns (7), (9) by substitution of the perturbed value of the energy into Eqn (6) instead of the unperturbed energy. This effect is taken into account in Refs [13, 14]. It should be noted that the perturbation theory is inapplicable in such strong fields, so it is necessary to calculate the AC Stark shift exactly. It was found that the ionization rate decreases approximately 1.5 – 2 times for a fixed value of the field strength, and the excitation curve has a lesser slope.

The ionization rates were derived numerically in Ref. [15] for the ground states of He and Li atoms with a constant electric field. The Hartree – Fock approximation was used for wave functions of these states. The results were compared with Eqn (9) for a circularly polarized field. Indeed, as we said above, the corresponding rates are of the same form as for a constant electric field. It was found that numerical calculations give rates lower than according to Eqn (9). Probably, the reason is that deviations from tunneling formula (9) already appear in relatively weak fields. Corrections for tunneling ionization rates are of the form of the factor $(1 + C_1 F + C_2 F^2 + \ldots)$, where the coefficients $C_1, C_2, \ldots$ of this asymptotic series are very large numbers. It follows from Ref. [15] that expressions for the tunneling ionization rates [including Eqns (2) and (3)] are valid up to values of the field strength which are much less than the atomic field strength. It will be seen below that this conclusion is in contradiction with experimental data. We do not presently know the reason for this contradiction.

The results obtained refer to a monochromatic electromagnetic field. In the case of a non-monochromatic field the instantaneous value of its intensity $I(t)$ may be higher or lower than the average value $\langle I(t)\rangle = I$. Due to the strong nonlinearity of the tunneling ionization process, large values of the intensity contribute more to the ionization rate than lower values (compared to average). Hence, the ionization rate by a non-monochromatic field is *greater* than by a monochromatic field for the same average intensity [16]. The factor for this amplification can be calculated for known distribution functions of laser intensity (see Ref. [17] for details).

4. Energy and angular distributions of photoelectrons in tunneling ionization

4.1 Linearly polarized radiation

The formulae of the previous section refer to the ionization rate integrated over all values of the energy and directions of ejected photoelectrons.

The expression for the rate of tunneling ionization for a fixed value of electron momentum **p** by linearly polarized radiation was obtained in Refs [18, 19]:

$$w(p_{\|}, p_{\perp}) = w(0)\exp\left[-\frac{p_{\|}^2\omega^2(2E_{\mathrm{i}})^{3/2}}{3F^3} - \frac{p_{\perp}^2(2E_{\mathrm{i}})^{1/2}}{F}\right]. \tag{10}$$

Here $p_{\|}$ and $p_{\perp}$ are the components of photoelectron momentum along and normal to the axis of polarization of laser field. The approach of Ref. [18] in the derivation of Eqn (10) is based on the *classical* motion of an electron in the vicinity of the maximum of the laser field strength:

$$F\cos\omega t \approx F\left(1 - \frac{\omega^2 t^2}{2}\right); \quad t \approx \frac{p_{\|}}{F}. \tag{11}$$

Thus, an electron obtains longitudinal momentum over the time t from the force F. Relations (11) are substituted into Eqn (7), and we obtain result (10). Oppositely, the approach of Ref. [19] is based on the *quantum mechanical* theory of strong adiabatic perturbations suggested by L D Landau and A M Dykhne (see Ref. [3] for details).

The exact value of the pre-exponential factor in Eqn (10) was obtained in Ref. [20] using the Keldysh – Faisal – Reiss method [21] and taking into account the Coulomb correction according to semiclassical perturbation theory:

$$w(0) = \frac{p\omega^2 D^2}{8\pi^3 n^* F}\exp\left[-\frac{2(2E_{\mathrm{i}})^{3/2}}{3F}\right]. \tag{12}$$

Here the quantity D is determined by relation (8). It is seen from Eqn (10) that the ionization rate has a maximum at zero electron energy, and decreases exponentially when this energy grows. According to Eqn (10) the width of the photoelectron energy spectrum is

$$\Delta E_{\|} = \frac{3F^3}{\omega^2(2E_{\mathrm{i}})^{3/2}} \ll \frac{F^2}{\omega^2}. \tag{13}$$

Thus, this width is small compared to the oscillation energy of an electron in the laser field (unlike the case of a circularly polarized field, see below).

According to Eqn (10), typical value of the transverse energy of a photoelectron is

$$\Delta E_{\perp} = \frac{F}{\sqrt{2E_{\mathrm{i}}}}. \tag{14}$$

Thus, it is small compared to the typical longitudinal energy (13), since the ratio of Eqn (14) to (13) is the square of the adiabaticity parameter (4).

It should be noted that after integration of Eqn (10) over all values of longitudinal and transverse photoelectron momenta we obtain Eqn (7), as expected.

Now we discuss the angular distribution of photoelectrons. It follows from Eqn (10) that it has sharp maximum in the direction of laser polarization, since $p_\perp = p\sin\theta \approx p\theta$; $\theta \ll 1$ is the angle between the direction of the ejected photoelectron and the polarization of a linearly polarized laser radiation. According to Eqn (10) the width of the angular distribution is

$$\Delta\theta = \frac{\sqrt{F}}{p(2E_i)^{1/4}}\,. \tag{15}$$

It should be noted that the dependence of Eqn (10) on the transverse momentum has the same form as for a constant electric field. The dependence of the distribution on the laser frequency appears only in the next order of approximation of the adiabaticity parameter (4):

$$w \propto \exp\left[-\frac{2}{3F}\left(\frac{1}{2}\,p_\perp^2 + E_i\right)^{3/2}\left(1-\frac{1}{10}\,\gamma^2\right)\right]. \tag{16}$$

The frequency correction is small even for an adiabaticity parameter of the order of unity; this allows tunneling expressions to be applied in the intermediate case between the tunneling and multiphoton limits.

Thus, it follows from Eqn (10) that the angular distribution of the photoelectrons in the low frequency linearly polarized field is of the form

$$w(\theta) = w(0)\exp\left[-\frac{p^2\sqrt{2E_i}}{F}\,\theta^2\right]. \tag{17}$$

The probability of ejection decreases exponentially with increasing angle θ. This conclusion is confirmed by experimental data (see below, Section 6.4).

4.2 Circularly polarized radiation

The maximum value of the ionization rate in the low frequency field of circular polarization occurs when the longitudinal energy is equal to the oscillation energy of a photoelectron in the field of circularly polarized electromagnetic wave (unlike the case of linear polarization where maximum value of the ionization rate takes place at zero energy, see the previous section):

$$E_{\|} \approx \frac{F^2}{2\omega^2}\,; \quad E_\perp = 0\,. \tag{18}$$

A nonzero value of the energy corresponds to circular motion of a photoelectron in a circularly polarized field.

The energy spectrum of ejected photoelectrons is of the form [18, 19] [instead of Eqn (10)]:

$$w = w_{\max}\sum_N \exp\left[-\frac{\omega^4\sqrt{2E_i}}{F^3}\,(N-N_0)^2\right]. \tag{19}$$

Here N is the number of absorbed photons of laser radiation , and the quantity

$$N_0 = \frac{F^2}{\omega^3} + \frac{4E_i}{3\omega} \approx \frac{F^2}{\omega^3} \tag{20}$$

corresponds to the number of photons in the case of the maximum ionization rate. The number of absorbed photons can be expressed via the kinetic energy E_e of the ejected photoelectron by a relation which follows from the energy conservation law:

$$N\omega = \frac{F^2}{2\omega^2} + E_i + E_e\,. \tag{21}$$

The first term in the right side of Eqn (21) represents the oscillation energy of the photoelectron in a circularly polarized field. This quantity is equal also to the positive AC Stark shift of the continuum edge. The maximum rate is achieved when the kinetic energy of the photoelectron is near the oscillation energy in the circularly polarized field.

The maximum value of the ionization rate in Eqn (19) was found in Ref. [20] in the framework of the Keldysh–Faisal–Reiss approach (the Coulomb correction was again calculated according to semiclassical perturbation theory):

$$w_{\max} = \frac{\omega^2 D^2}{8\sqrt{\pi^3 n^* ZF}}\exp\left[-\frac{2(2E_i)^{3/2}}{3F}\left(1-\frac{1}{15}\,\gamma^2\right)\right]. \tag{22}$$

The correction in this expression depending on the frequency corresponds to the deviation from the tunneling regime (analogously to the case of linear polarization discussed in the previous section). It should be noted that the pre-exponential factor strongly increases the tunneling ionization rate.

An important peculiarity of the ionization in a circularly polarized field is that most of the photoelectrons are ejected in the polarization plane. The radius of the electron orbit in this plane F/ω^2 is large compared to the size of an atom, but, of course, it is small compared to the radius of the laser focusing region. The number of electrons ejected at an angle ψ is determined by the relation

$$w(\psi) = w(0)\exp\left[-\frac{F\sqrt{2\,E_i}}{\omega^2}\,\psi^2\right]. \tag{23}$$

The width of this angular distribution is

$$\Delta\psi = \frac{\omega}{\sqrt[4]{2E_iF^2}}\,. \tag{24}$$

The exponential decrease of the ionization rate with increasing angle is confirmed by experimental data (see Section 6.4).

4.3 Ponderomotive acceleration of photoelectrons

The classical motion of an electron in an alternating electromagnetic field can be presented as superposition of rapid oscillations with small amplitude and slow drift due to spatial dependence of the laser intensity in the focusing volume. We underline once more that this amplitude F/ω^2 is always small compared to the focusing radius R.

The results obtained above refer to the case when the electron coordinate is not shifted essentially during the laser pulse duration t_l. This means that the electron path is $L = v\,t_l \ll R$, where v is the electron velocity. Such a situation is realized for ultrashort laser pulses with durations of picoseconds and less.

In the opposite limiting case of long laser pulses an electron is accelerated by a spatial gradient of the laser field in the direction perpendicular to the laser beam. Thus, the electron's direction is changed after the ionization process. The corresponding force is called the *ponderomotive force* (or

gradient force). The electron's acceleration is called *ponderomotive acceleration*. The ponderomotive force is of the form (in the case of a linearly polarized field)

$$\mathbf{j} = -\nabla\left[\frac{F^2(\mathbf{r}, t)}{4\omega^2}\right]. \tag{25}$$

The right side of this expression should be multiplied by two in the case of a circularly polarized field.

Ponderomotive acceleration changes only the angular and energy distributions of photoelectrons, but the total ionization rate is not varied. The kinetic energy which a photoelectron obtains in a long pulse is

$$E_e = \frac{F^2(\mathbf{r}_0, t_0)}{4\omega^2}. \tag{26}$$

Here the quantities r_0, t_0 are the radius-vector and the moment of ionization in the focusing volume, respectively. Since the values of the field strength on the right side of Eqn (26) vary in the focusing volume, there is some photoelectron distribution of kinetic energies which is weighted with a different probability of production at various points. Of course, the average kinetic energy is *larger* than the mean value of the right side of Eqn (26) because of strong nonlinearity of the tunneling ionization process.

In the intermediate case $L \sim R$ the kinetic energy of a photoelectron after leaving the laser focus can be derived only numerically [22]. Calculations had been made for Gaussian and more realistic envelopes of the radiation intensity in the focusing volume. It should be noted that above considerations refer only to the average part of the kinetic energy. Rapid oscillations of an electron with a small amplitude are produced by the instantaneous value of the field strength: they deplete slowly to zero when this electron goes out of the laser focusing volume. The total electron kinetic energy is the sum of the ponderomotive energy and the kinetic energy obtained by this electron in the ionization process according to the energy distributions (10), (19). The maximum value of the kinetic energy is achieved for electrons ejected from the center of the laser focus. The distribution over the final kinetic energies was calculated in Refs [23, 24] for the case of linearly polarized radiation. The approximation was made that the spatial distribution of laser radiation is of a Gaussian form in the direction perpendicular to the direction of the laser beam. This distribution has the analytical form

$$w(E_e) = w(E_p)\exp\left[-4\frac{\omega^2(2E_i)^{3/2}}{3F^3}(E_p - E_e)\right],\ E_e < E_p;$$
$$w(E_e) = w(E_p)\exp\left[-2\frac{\omega^2(2E_i)^{3/2}}{3F^3}(E_e - E_p)\right],\ E_e > E_p. \tag{27}$$

Here the maximum ponderomotive energy is determined by the maximum values of the radiation field strength in the center of the laser focusing volume:

$$E_p = \frac{F_{max}^2}{4\omega^2}. \tag{28}$$

Let us underline once more that the distribution (27) is valid for long laser pulses. The position of the peak of the spectrum is determined by the maximum value of the ponderomotive energy. It is seen that distribution (27) is asymmetrical with respect to its maximum. The width of the distribution (27) is small compared to the energy (28) at maximum, i.e. this peak is rather narrow. The spread of the peak is determined by photoelectrons with nonzero initial kinetic energies, i.e. it is of the order of the width (13).

Experimental electron spectra for the ionization of Xe atoms [25] are in good agreement with the above theoretical expressions, if the (negative) AC Stark shift of the ground state is taken into account. In this case the AC Stark shift coincides with the static Stark shift due to the low laser frequency. This effect shifts the position of the maximum in the energy spectrum due to the change in the count off for the photoelectron kinetic energy.

Let us discuss briefly the angular distribution of photoelectrons in the case of long laser pulses. In the case of linear polarized radiation, most of the electrons are ejected in the plane perpendicular to the laser beam, while immediately after ionization they are ejected along the direction of the laser polarization. In the case of circular polarized radiation the duration of the laser pulse does not influence the angular distribution: electrons are always ejected in the plane perpendicular to the laser beam; besides this, the angular distribution is axially symmetric.

4.4 Return of ejected electrons to the atomic core

We assumed above that after leaving the effective potential barrier an electron goes to infinity. In fact, this is correct only in the case of a constant electric field. In the field of laser radiation an electron oscillates; hence, it returns to the atomic core and scatters after approximately half the radiation period. Of course, such a process occurs if the initial electron's velocity after leaving the effective potential barrier is zero, so that this electron does not have any drift velocity.

We will consider the electron's motion outside the potential barrier in the framework of classical mechanics, neglecting the spreading of the corresponding quantum mechanical wave packet. During the classical motion the electron can acquire some energy from the external electromagnetic field. The value of this energy depends on the field phase when the electron leaves the barrier. Such an effect was first suggested by Kuchiev [26] and investigated in detail in Refs [27 – 31].

After elastic scattering on the atomic core the electron goes to infinity with the excess energy from the external field. In principle, multiple scattering is also possible; however, the probability is small, from the practical point of view.

Besides scattering, after returning the electron can recombine into the initial binding atomic state. The excess energy is lost through the ejected photon. We do not consider this process in detail. Finally, the returning electron can inelastically scatter on the atomic core with ejection of the second electron. Since the energy of the returning electron may be of the order of the oscillation energy of the electron in the field of the electromagnetic wave, in the tunneling regime this is much more than the ionization potential of the atomic core. Thus, the second electron may obtain an energy much greater than the ionization potential; in this case the *above-threshold ionization* of both electrons occurs. It is accompanied by the absorption of many more photons than required for ionization according to the energy conservation law.

Let us calculate the energy which may be obtained by an electron from the electromagnetic field in returning to the atomic core. It should be noted that this problem is reason-

able only in the tunneling regime. In the opposite case of multiphoton ionization when the adiabaticity parameter $\gamma \gg 1$, the amplitude of electron oscillations F/ω^2 is small compared to the length E_i/F for which the electron is under the potential barrier. Consequently, in this case we can neglect classical oscillations outside the barrier.

Besides this, we consider the case of *linear* polarization of laser radiation only. Obviously, the classical rescattering of an electron is impossible in the field of circularly or elliptically polarized radiation. For simplicity, in this section, the charge and mass of an electron are chosen to be equal to unity.

The one-dimensional Newton equation for the motion of a free electron along the polarization axis after leaving the effective potential barrier is of the form

$$a(t) = -F\sin(\omega t + \varphi)\,. \tag{29}$$

Here $a(t)$ is the electron's acceleration, φ is the initial phase of the electromagnetic field, and F, ω are the field strength amplitude and field frequency, respectively.

Integrating Eqn (29), we obtain the electron's velocity as a function of time:

$$v(t) = v(0) + \frac{F}{\omega}\left[\cos(\omega t + \varphi) - \cos\varphi\right]. \tag{30}$$

Here $v(0)$ is the electron's velocity for the initial moment $t = 0$ when the electron leaves the effective potential barrier. Further we put $v(0) = 0$ for the tunneling quasi-static process.

Integrating Eqn (30), we obtain the electron's coordinate as a function of time:

$$x(t) = x(0) + \frac{F}{\omega^2}\left[\sin(\omega t + \varphi) - \sin\varphi\right] - \frac{Ft}{\omega}\cos\varphi\,. \tag{31}$$

Here $x(0)$ is the initial electron coordinate.

In tunneling regime the oscillation amplitude of an electron F/ω^2 is large compared to the coordinate E_i/F of the right classical turning point (this is the point where an electron is going out of the barrier). Hence, we can approximately put $x(0) = 0$.

At some time $\tau > 0$ the electron returns to the atomic core. Thus, we again have $x(\tau) = 0$. According to Eqn (31) we find the equation

$$\sin(\omega\tau + \varphi) - \sin\varphi = \omega\tau\cos\varphi\,. \tag{32}$$

Our goal is to derive the electron's velocity for the moment of return $v(\tau)$. This quantity is a function of the phase φ. We calculate the maximum value of this velocity only. The condition for maximum is

$$\frac{\mathrm{d}v(\tau)}{\mathrm{d}\varphi} = 0\,. \tag{33}$$

Substituting Eqn (30) into (33), we obtain

$$\left(\omega\frac{\mathrm{d}\tau}{\mathrm{d}\varphi} + 1\right)\sin(\omega\tau + \varphi) = \sin\varphi\,. \tag{34}$$

From the other side, differentiating Eqn (32) on φ, we have

$$\left(\omega\frac{\mathrm{d}\tau}{\mathrm{d}\varphi} + 1\right)\left[\cos(\omega\tau + \varphi) - \cos\varphi\right] = -\omega\tau\sin\varphi\,. \tag{35}$$

Dividing Eqn (35) by (34) we obtain an equation which does not contain derivatives:

$$\cos(\omega\tau + \varphi) - \cos\varphi = -\omega\tau\sin(\omega\tau + \varphi)\,. \tag{36}$$

It follows from the algebraic system of equations (32) and (36) that

$$4\varphi = -\pi - 2\omega\tau\,. \tag{37}$$

Substituting Eqn (37) back into (32), we find the equation for the returning time:

$$\omega\tau(1 + \cot\omega\tau) = 1\,. \tag{38}$$

A numerical solution of this transcendental equation is $\omega\tau = 4.08556$. Then it follows from Eqn (37) that $\varphi = -1.25739$. It should be noted that the returning time is somewhat greater than half of the field period of the laser radiation.

Substituting the values obtained for $\omega\tau$, φ into Eqn (30), we find the maximum velocity of an electron when it returns to the atomic core:

$$E_{\max} = \frac{1}{2}v_{\max}^2(\tau) = \frac{F^2}{2\omega^2}\left[\cos(\omega\tau + \varphi) - \cos\varphi\right]^2 \approx 3.173E_p\,, \tag{39}$$

here $E_p = F^2/4\omega^2$ is the maximum ponderomotive energy of an electron in the linearly polarized field. This result was obtained first in Ref. [30]. It is seen that due to the effect of returning an electron may acquire an energy of the order of the ponderomotive energy, while the average energy of an electron without returning is much less than the ponderomotive energy [see Ref. (13)].

On the assumption that the field phase takes random values, the energy distribution of electrons after returning to the atomic core was obtained in Ref. [32]. It was found that a very sharp peak occurs near $E_{\max}$. It was also obtained that the electron's return is impossible for field phases in the interval $0 < \varphi < \pi$. Thus, approximately half of the electrons return to the atomic core in half of the field period of the laser radiation.

The conclusion can be made that the effect of returning influences the energy distribution of electrons at the tunneling ionization, producing hot electrons. However, the number of such electrons is very small. Moreover, the value of Eqn (39) is the maximum electron energy only in the process of harmonic generation; in this case the electron recombines into the ground state of an atom with the emission of a spontaneous photon having the energy (39). Besides this, rescattering of the electron on the atomic core is possible. After rescattering the laser radiation can also give energy to this electron. The maximum value of the energy (of the order of $10E_p$) is achieved when the electron is moving back after rescattering (backscattering) [33].

The return of the electron can also be described quantum mechanically using the Keldysh–Faisal–Reiss approach. This approach uses the first order perturbation theory on the potential of the atomic core, an unperturbed initial binding atomic state and a Volkov wave function for the final continuum state. The exact transition amplitude can be written using the second iteration on the potential of the atomic core. In the approximation that the electron is moving in the intermediate state in the field of the electromagnetic wave only, and that its final wave function is again a Volkov

function, in Ref. [34] the electron energy spectrum was calculated for a helium atom. The energy spectrum obtained contains hot electrons as well with energies up to $10E_p$. Thus, quantum mechanical calculations confirm the results of the simple classical theory described above. However, the Coulomb correction is not taken into account in [34]; a zero-range potential was used as the potential of the atomic core.

5. Barrier-suppression ionization

The classical expression (5) corresponds to a step-wise classical dependence of the ion yield on the electric field strength of the low frequency laser radiation: the yield is zero for $F < F_{BSI}$; otherwise all atoms are ionized. However, such a classical model is too simplified. In this section the quantum mechanical approach of Ref. [20] for barrier-suppression ionization is developed; it also includes the tunneling ionization considered above as the limiting case of a weak laser field. Thus, this approach should make the step-wise dependence smoother. We use the Keldysh – Faisal – Reiss method [21] which does not have a restriction on the laser field from above, unlike the Keldysh theory [1]. Besides this, the Coulomb correction for the Volkov wave function of the final continuum state is taken into account. The conclusion is that the extrapolation of tunneling expressions into the region of critical fields F_{BSI} overestimates the ionization rate (see Fig. 3). The dependence of the ionization rate on the field strength is still smoother at large field strengths.

In this section the role of the Stark shift of the initial binding state is discussed for the problem considered. It follows from numerical calculations for the hydrogen atom that the values of the Stark shift diminish strongly with increasing field strength compared to predictions based on the second order perturbation theory.

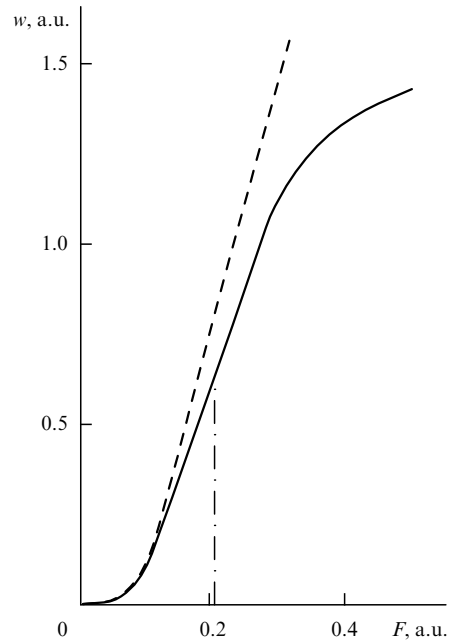

Figure 3. Barrier-suppression ionization rate for the ground hydrogen state by low frequency circularly polarized radiation according to the calculations of Ref. [35]. The dotted line is the result of the tunneling expression (2).

Though tunneling ionization in a constant electric field is only possible in the framework of quantum mechanics, barrier-suppression ionization is a classical threshold effect. Tunneling ionization in a low frequency variable field is possible, in principle, in the framework of classical mechanics, but for a small set of initial values of the trajectory parameters (this is the so called Arnold diffusion [36]); this process is not described by any analytical dependencies.

5.1 Coulomb correction

The Keldysh – Faisal – Reiss method is based on the S-matrix approach; the final electron state is supposed to be a state of a free electron in the field of laser radiation. The Coulomb potential of the atomic, or ionic core is taken into account in the framework of semi-classical perturbation theory as a small correction to the classical action [20, 35]. The transition amplitude from the initial binding state i to the final continuum state f is described by an element of the S-matrix:

$$A_{if} = -i \int \langle \Psi_f^{(V)} I | V(\mathbf{r}, t) | \Psi_i^{(0)} \rangle \, dt . \tag{40}$$

Here

$$V(\mathbf{r}, t) = \frac{1}{c}(\mathbf{p} \cdot \mathbf{A}) + \frac{1}{2c^2} \mathbf{A}^2$$

is the interaction potential between the atomic system and the external electromagnetic field in the velocity gauge, which is taken into account in the dipole approximation. The Coulomb correction I is determined below. The Volkov wave function of the final continuum state calculated in the same gauge is

$$\Psi_f^{(V)}(\mathbf{r}, t) = \exp\left\{ -i(\mathbf{p} \cdot \mathbf{r}) + \frac{i}{2} \int^t \left[\mathbf{p} + \frac{1}{c} \mathbf{A}(t') \right]^2 dt' \right\} .$$

For simplicity we suggest first that the initial binding state is an s-state. Then we will consider other values of the initial angular momentum. The unperturbed wave function of the initial binding state is of asymptotic form [at distances which are large compared to the size of the atomic system: just these distances are important in the integral of Eqn (40)]:

$$\Psi_i^{(0)}(\mathbf{r}, t) = \sqrt{\frac{Z^3}{8\pi^2}} \left(\frac{2e^2}{\pi} \right)^{n^*} (Zr)^{n^*-1} \exp\left(-\frac{Zr}{n^*} + iE_i t \right) .$$

Here the Stirling formula has been used for the factorial of the effective principal quantum number $n^* \equiv Z/\sqrt{2E_i}$; Z is the charge of atomic or ionic core.

The Coulomb correction to the Volkov wave function is determined in the framework of semi-classical perturbation theory with respect to the Coulomb potential $U = -Z/r$. We find

$$I = \exp\left(-i \int U \, dt \right) . \tag{41}$$

Further we change the integration over time for integration over the radial coordinate, using the obvious relation

$$dt = \frac{dr}{p} = \frac{dr}{\sqrt{(Z/n^*)^2 - 2Fr}} .$$

Here p is the radial momentum of the electron. We neglect here the centrifugal energy and also the contribution of the

Coulomb potential to this momentum, since we restrict ourselves to first order semi-classical perturbation theory with respect to the Coulomb potential.

The upper limit of integration over the radial coordinate in Eqn (41) is the right classical turning point where $p(r_0) = 0$, since larger distances change the constant phase of the transition amplitude only. The lower limit of integration is some arbitrary value of r which satisfies two conditions restricting this value from above and below. This quantity is restricted from above by the condition that in this region we can neglect the external electric field, i.e. $Fr \ll E_i$. It is restricted from below by the condition that we use an asymptotic expression for the unperturbed wave function of the initial binding state, i.e. $r \gg n^{*2}/Z$. Both inequalities can be strictly fulfilled in the case of tunneling ionization. However, in the case of barrier-suppression ionization all quantities are of the same order of magnitude, so that the pre-exponential factors obtained in the rate for barrier-suppression ionization are of semi-quantitative accuracy only.

It should be noted that though the low frequency field of the electromagnetic radiation is a variable, we consider in the derivation of the Coulomb correction only the maximum value of the field strength, since the ionization rate is nonzero only in the vicinity of this maximum value.

After calculation of the simple integral in Eqn (41) we obtain the Coulomb correction in the form [20]

$$I = \left(\frac{2Z^2}{n^{*2}Fr}\right)^{n^*} . \tag{42}$$

Integration of expression (40) by parts simplifies its form [21]:

$$A_{if} = i\left(\frac{1}{2}p^2 + E_i\right)\int \left\langle \Psi_f^{(V)} | I | \Psi_i^{(0)} \right\rangle dt . \tag{43}$$

Further we present the results of calculations for circularly and linearly polarized fields.

5.2 Circularly polarized radiation

The vector potential of circularly polarized radiation is written in the form

$$\mathbf{A} = \frac{cF}{\omega}(\mathbf{i}_x \cos\omega t + \mathbf{i}_y \sin\omega t) .$$

Here the basic vectors along the x and y axes are introduced. Substituting this expression into the Volkov wave function contained in Eqn (43), we calculate the transition amplitude and then the ionization rate. Recall that we assume the energy of a photon of laser radiation is small compared to the binding potential of the atomic system considered, and the field strength is of the order of the critical field strength (5). After calculations we obtain the energy and angular distribution of the ejected photoelectrons:

$$\frac{dw}{d\Omega} = \frac{\omega Z D^2}{(2\pi n^*)^2 \sqrt[3]{2F}} \times Ai^2\left[\frac{2E_i + (F\psi/\omega)^2 + \omega^4(N - N_0)^2/F^2}{(2F)^{2/3}}\right] . \tag{44}$$

Here N is the number of absorbed photons of laser radiation which determines the kinetic energy of the ejected photoelectron according to the energy conservation law (21). The quantity N_0 corresponds to the maximum value of the ionization probability; it is determined by Eqn (20). The quantity ψ is the small angle between the direction of the ejected photoelectron and the polarization plane of the laser radiation. Finally, $Ai(x)$ is the Airy function. Equation (44) reduces to the energy and angular distributions for tunneling ionization (19) and (23) in the tunneling limit of a weak field.

The width of the energy spectrum having the maximum at the kinetic energy of the electron $F^2/2\omega^2$ (this is the oscillation energy in the field of circularly polarized radiation) according to Eqn (44) is

$$\Delta E_e = \frac{F^{3/2}}{\omega\sqrt[4]{2E_i}} .$$

The spectral width increases with growing field strength. Thus, the energy spectrum for barrier-suppression ionization is broader than for tunneling ionization.

Integrating Eqn (44) over all energies (i.e. summing over all numbers of absorbed photons in the vicinity of N_0) and angles of ejected photoelectrons, we obtain the rate for barrier-suppression ionization by circularly polarized radiation:

$$w_{BSI} = \frac{ZD^2\sqrt[3]{2F}}{2n^{*2}}\left[\left(\frac{dAi(k)}{dk}\right)^2 - kAi^2(k)\right] . \tag{45}$$

Here the notation is introduced

$$k \equiv \frac{2E_i}{(2F)^{2/3}} . \tag{46}$$

We can take into account the Stark shift of the initial binding state by means of the change $E_i \to E_i(F)$ where the perturbed binding energy is found from the unperturbed energy by addition of the AC Stark shift in all orders of the perturbation theory. Due to the smallness of the radiation frequency this AC Stark shift can be considered as a static Stark shift. However, numerical calculations for the Stark shift from the framework of the lowest approximation of the perturbation theory are known only for the hydrogen atom [37]. In this case it was found that at a field strength ten times less than the critical value (5), the Stark shift differs strongly from the quadratic Stark shift. For a further increase of the field strength, the value of the Stark shift is much less than the extrapolation of the quadratic Stark shift into this region of critical fields. For this reason, probably, it is better to neglect the Stark shift in the above expressions than to substitute the values of the quadratic Stark shift and to extrapolate them into the region of critical fields.

Using the known asymptotic properties of the Airy function and of its derivative, we can obtain the ADK formula (9) from Eqn (45) in the limit of a weak field ($k \gg 1$), as expected. In the case of ground state of hydrogen atom we obtain the well-known formula (2) from Eqn (45) in the limit of a weak field with an accuracy of 18% (the difference is explained by application of the Stirling formula for 1!).

In Figure 4 the ratio of the rate for barrier-suppression ionization derived according to Eqn (45), to the rate for tunneling ionization derived according to the ADK formula (9) is shown as a universal function of the universal parameter k (46). The conclusion can be made that the rate for barrier-suppression ionization is less than the extrapolation of the rate for tunneling ionization into the above-barrier region.

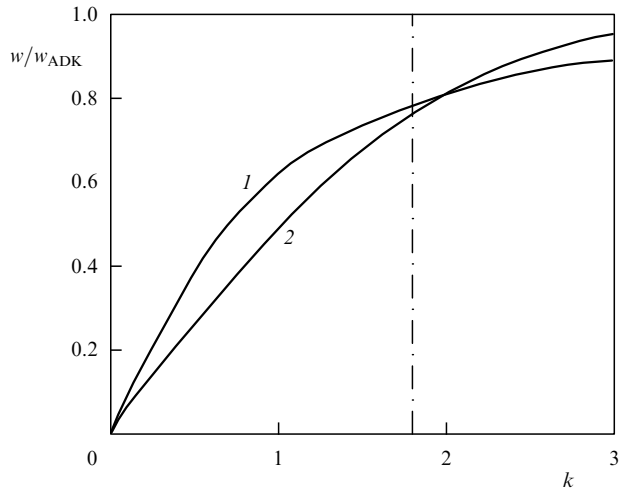

Figure 4. Ratio of the barrier-suppression ionization rate [20] to the tunneling ionization rate (ADK formula) as a function of the universal parameter k: (*1*) circular polarization, (*2*) linear polarization.

The larger the field strength, the stronger the difference between the rates.

Numerical calculations of the ionization rate in a constant electric field with a field strength of the order of value (5) and higher were reported in Ref. [37] for the ground and some excited states of a hydrogen atom.

In Figure 5 the dependence of the ionization rate for the ground state of a hydrogen atom is shown as a function of the strength of the constant electric field. It was found in comparison with Eqn (45) that the numerical values are 5–8 times less than according to Eqn (45) in the region of critical fields. Thus, the conclusion can be made that both the tunneling ADK expressions and the above expressions for barrier-suppression ionization *overestimate* the correct value of the ionization rate.

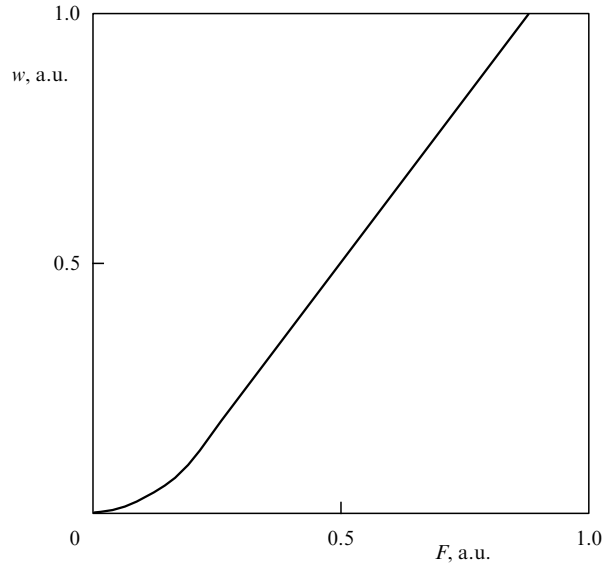

Figure 5. Ionization rate of the ground state of a hydrogen atom by a constant electric field as a function of the field strength according to the calculations of Ref. [37].

Here we have considered the ionization from the binding state with zero angular momentum. p-states are also of practical interest (atoms and ions of noble gases). It follows from analysis of the pre-exponential factor in Eqn (6) that the main contribution to the ionization rate is given by the initial sub-state with the magnetic quantum number $m = 0$. The ionization rates of sub-states with $m = +1$ and -1 are much less. These statements are valid both for tunneling and barrier-suppression ionization. Further, it follows from Eqn (6) that the ionization rate from the p-state with $m = 0$ is three times larger than that from the s-state. Therefore the ionization rate of the p-state averaged over all magnetic quantum numbers (this procedure is correct when all sub-states are equipopulated) is equal to the ionization rate of the s-state, i.e. to Eqn (45). The same conclusion can also be made for initial atomic states with arbitrary angular momenta.

5.3 Linearly polarized radiation

The vector potential of a linearly polarized electromagnetic field is written in the form (in dipole approximation)

$$\mathbf{A} = -\frac{c\mathbf{F}}{\omega}\sin\omega t\,.$$

Substituting this expression into the Volkov wave function contained in the amplitude (43) we calculate this amplitude and then the square of its modulus. Thus, we obtain the energy and angular distribution of ejected electrons . Again we consider the case of initial an s-state and assume that the energy of a photon of laser radiation is small compared to the ionization potential of the atomic state considered, and also that the field strength is of the order of the critical value of Eqn (5). Details of the calculations can be found in Ref. [20]. Unlike the case of circular polarization, the expansion of the Volkov wave function in a Fourier series is impractical, since in the general case of arbitrary values of the adiabaticity parameter it gives the generalized Bessel functions [21]. Direct calculation of Eqn (4) by the saddle-point method gives the distribution of ejected photoelectrons on the longitudinal momenta $p_{\|}$ and on the transverse momenta $p_{\perp}$ with respect to the direction of polarization of laser radiation and is of the form

$$\frac{\mathrm{d}w}{\mathrm{d}\Omega} = \frac{p\omega^2 ZD^2}{(\pi n^*)^2(2F)^{4/3}}\,Ai^2\left[\frac{2E_\mathrm{i} + p_\perp^2 + F\gamma^3 p_{\|}^2/(3\omega\sqrt{2E_\mathrm{i}})}{(2F)^{2/3}}\right]. \tag{47}$$

Here the transverse momentum can be expressed via the small angle θ between the direction of the ejected electron and the polarization of laser radiation: $p_\perp = p\sin\theta = p\theta$. The quantity D is determined by relation (8), and the adiabaticity parameter is determined by relation (4).

Expression (10) follows from Eqn (47) in the tunneling limit, as expected (with correct pre-exponential factor). Analogously to the case of tunneling ionization, the energy spectrum of barrier-suppression ionization has a maximum for zero kinetic energy of the electron.

Integrating Eqn (47) over all energies and angles of the photoelectron, we obtain the ionization rate for barrier-suppression ionization by a linearly polarized field:

$$w_\mathrm{BSI} = \frac{4\sqrt{3}FD^2}{\pi n^*\sqrt[3]{2F}}\int_0^\infty Ai^2\left[x^2 + \frac{2E_\mathrm{i}}{(2F)^{2/3}}\right]x^2\,\mathrm{d}x\,. \tag{48}$$

This expression reduces to the ADK formula (7) in the tunneling limit of a relatively weak field, as expected.

In Figure 4 the ratio of expression (48) to expression (7) is shown as a function of the parameter k (46). The conclusion can be made that the rate for barrier-suppression ionization is *less* (as in the case of circular polarization) than the extrapolation of the tunneling ADK expression into the region of critical fields. Again the difference grows with increasing field strength.

It should be noted in conclusion that these simple expressions are also applicable for molecular systems.

The energy and angular distribution of ejected electrons in the tunneling ionization of atomic systems by a field of elliptical polarization was considered in Ref. [38]. The Volkov wave function of the final continuum state also was not expanded in a Fourier series; instead, the integrals in the transition amplitude were derived by the saddle-point method. The Coulomb correction was not taken into account, so that only the exponent is correct in the expressions obtained. The dependence of this exponent on the degree of ellipticity was found analytically.

6. Experimental data and interpretation

6.1 Experimental values of the adiabaticity parameter

It follows from the results of the previous section that tunneling ionization takes place under the conditions $\gamma^2 \ll 1$ and $F \ll F_{\mathrm{BSI}}$. The adiabaticity parameter γ is defined by relation (4). This parameter first appeared in the problem of ionization of a particle bound by zero-range forces. The applicability of this parameter for atoms and positive ions follows both from experimental data and from calculations.

Some experiments [2, 39] confirm this conclusion. The radiation frequency is fixed in these experiments, and the radiation intensity varied. The ionization of atoms of noble gases has been observed, and the electron energy spectra have been measured. It is found that resonance maxima in the spectra occur at $\gamma > 1$ and disappear at $\gamma < 1$. Resonance maxima describe the above-threshold absorption of photons for multiphoton ionization (see Ref. [10] for details) and also resonances with high excited atomic states. Smooth energy spectra correspond to the tunneling regime of ionization. In Figure 2, typical results of the experiment reported in Ref. [2] are shown. It is seen, in particular, that tunneling ionization takes place at $\gamma \sim 1$. This conclusion is in agreement with the above theoretical considerations. It should be noted that the transition from tunneling to multiphoton ionization occurs over a narrow range of variation of laser intensity. It is partially explained by the fact that the ionization rates depend on the quantity γ^2 .

6.2 Ion yield in tunneling ionization

The first attempts to observe tunneling ionization were made in Refs [40–42]. In these experiments atoms were irradiated by a Nd:glass laser. The dependence of the ion yield on the radiation intensity was measured for the atoms of several noble gases. Helium and neon ions appear for an adiabaticity parameter of $\gamma = 0.3-0.5$. The authors of Refs [40, 42] suggested that multiphoton ionization occurred. The authors of Ref. [41] gave arguments for tunneling ionization. It should be noted that it is very hard to differ tunneling ionization from multiphoton ionization for high nonlinearity because of the limited intensity range in those experiments.

Systematic investigation of the process of tunneling ionization began in 1983 [43] (see the historical review in Ref. [8]). The yields of ions of gases were measured for irradiation by an IR CO_2-laser of wavelength 10 μm. The adiabaticity parameter γ and the amplitude of the field strength were, respectively: K atoms — $\gamma = 0.3$, $F = 0.01$ a.u. [25]; Xe atoms — $\gamma = 0.01$, $F = 0.05$ a.u. [7]; Hg atoms — $\gamma = 0.03$, $F = 0.01$ a.u. [44]. In Figure 6 the typical dependencies of ion yields on the intensity of laser radiation (the so called *excitation curves*) are shown. A comparison of experimental data with the results of calculations according to the tunneling ADK expressions [12] (see Section 2) demonstrates a good agreement in most cases.

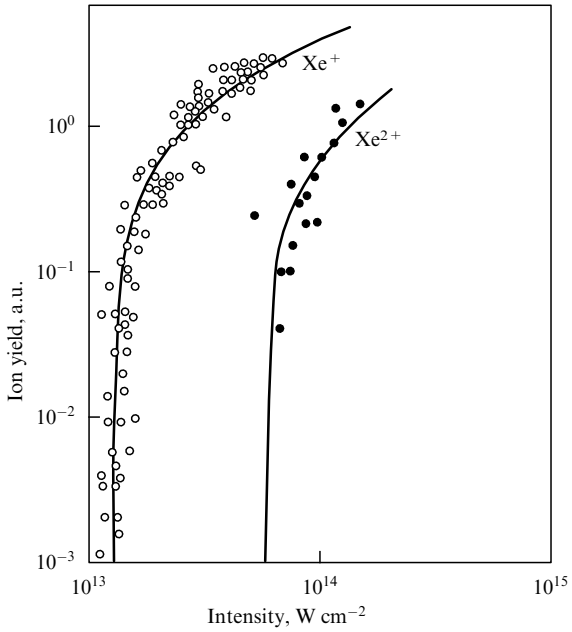

Figure 6. Yield of Xe^+ and Xe^{2+} ions as a function of the intensity of the CO_2-laser according to experimental data [25]. The solid lines represent the result of the calculations by the ADK approach.

A large amount of experimental data with radiation of IR, visible and near UV ranges was obtained in other experiments at $\gamma < 1$, $F \sim 0.1$ a.u. [45–49]. These data are also in good agreement with the predictions of the ADK approach.

Linearly polarized laser radiation was used in all above cited works. Circularly polarized radiation was used in the experiments reported in Refs [46, 48]. The ratio of the ion yield for circular polarization to the ion yield for linear polarization of radiation was measured in Ref. [50]. The ionization of Ar atoms using radiation of a Ti–Sapphire laser with a pulse length of 200 fs was considered. It was found that this ratio increases with increasing radiation intensity. The measured ion yields are in good agreement with the predictions of the ADK approach, though the values of the adiabaticity parameter were of the order of unity or a little less. The field strength for circular polarization is $\sqrt{2}$ times less than for linear polarization at the same laser intensity. On the other hand, a circularly polarized field acts instantaneously, unlike a field of linear polarization. This produces a difference in the pre-exponential factors of the ADK expressions (7) and (9). This difference is of the order of 2 in the case of the experiments of Ref. [48] for Xe and Ar atoms. An intensity one and a half times higher is needed for the

ionization of these atoms by a circularly polarized field compared a linearly polarized field. This theoretical conclusion was confirmed experimentally [48].

6.3 Production of multicharged ions

The production of multicharged ions was observed in some experiments with atoms of noble gases irradiated by light in the visible and near IR ranges at $\gamma < 1$ and $F < F_{\mathrm{BSI}}$. The excitation curves for doubly-charged ions correspond to a cascade process of ionization (see Ref. [3]):

$$\mathrm{A} + K_1\omega \to \mathrm{A}^+; \quad \mathrm{A}^+ + K_2\omega \to \mathrm{A}^{++}\,.$$

Doubly-charged ions are observed at the radiation intensity for which the saturation of yields for single-charged ions occurs: the total ionization probability $W = wt_1 \sim 1$, where w and t_1 are the ionization rate and duration of the laser pulse, respectively. Excitation curves for the yield of doubly-charged ions are described well by ADK expressions both for linear and circular polarization. These experimental data were obtained in Refs [47–49, 51]. A typical excitation curve is shown in Fig. 7. Qualitative forms of the excitation curves and a quantitative agreement between experimental data and predictions of ADK approach confirm the assumption about the cascade mechanism for the production of doubly-charged ions. Besides this, such an agreement permits us to conclude that the ADK expressions are also applicable for ionization of positive charged ions with multiplicities up to $q = 8$ [49].

It should be noted that while cascade ionization was observed in some experiments [47–49, 51], a strong deviation from the cascade process took place in other experiments [39, 45, 52–55], though approximately the same values of the radiation intensity and of the adiabaticity parameter were realized in all experiments. Typical excitation curves are shown in Fig. 8. It is seen that the experimental values of ion yields are essentially higher than the estimates according to the ADK expressions for low radiation intensity. The theoretical and experimental dependencies coincide only at moderate and high laser intensities. Two models of *direct* ionization (simultaneous detachment of two electrons) at low radiation intensity were suggested to explain this effect:

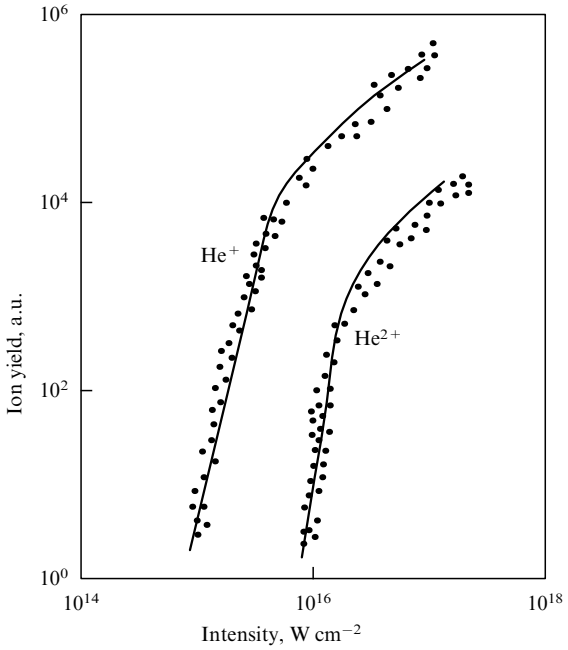

Figure 7. Yield of singly-charged and doubly-charged ^{3}He ions as a function of the intensity of laser radiation according to the experimental data of Ref. [51]. The solid lines represent results of calculations by the ADK approach.

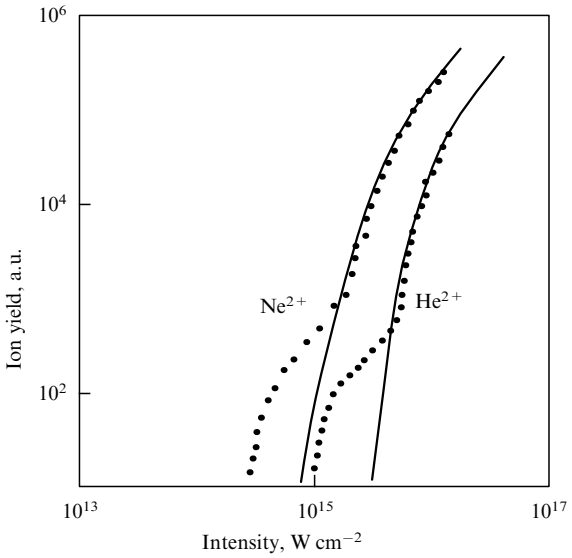

Figure 8. Yield of doubly-charged He and Ne ions versus the intensity of linearly polarized laser radiation according to the experimental data of Refs [52, 54]. The solid lines are the results of calculations by the ADK approach.

1. **'Shake-off' model** [52]. The first electron quickly leaves the region near of the atomic core producing the 'shake-off' of the second electron; this process takes place over a quarter of a laser period, or less. The ionization of the second electron occurs due to the sudden change of the effective potential of the atomic core in the production of a new ionic potential, when the first electron is leaving [56]. The wave function of the second electron does not change in this process; its overlap with the wave functions of the continuum spectrum of the new basis determines the ionization amplitude.

2. **Rescattering model** (see above, Section 4). The first ejected electron interacts with the field of laser radiation; approximately half of the electrons return to the parent ion over approximately half of the optical period. The returning electron ionizes the second electron by means of inelastic scattering, since the returning electron can obtain a large energy from the external electromagnetic field (of the order of its oscillation energy).

The strong dependence of the ion yield on the polarization of the laser radiation observed in Ref. [54] is in agreement with the second model: this effect is observed for a *linearly* polarized field only. At present we cannot make any single-valued conclusion from the results obtained.

Besides this, it is unclear why the effect takes place for low radiation intensity only where strong deviations from ADK expressions occur. It is also unclear why this effect exists for one kind of atoms while it is absent for other atoms.

Thus, the experimental data do not allow us to make some conclusions about why the ion yield increases compared to the predictions about the cascade mechanism of ionization. It is unclear why the models of shake-off and rescattering are applicable for weak fields and inapplicable for strong fields.

It is possible that the rise of the ion yield at relatively low laser intensity can be explained by the fact that these ions are produced on the borders of the laser focusing volume where the adiabaticity parameter is larger than unity. Then the multiphoton resonance process of ionization (with high excited atomic states) may be realized in this region. Of course, such a model is very sensible to the details of the experiment: the spectrum of atomic states, the radiation frequency, the AC Stark shift, and the spatial-temporal distribution of the intensity of laser radiation. The observed effects may be explained by such details.

One more explanation was suggested in Ref. [57]. The rate for nonlinear simultaneous two-electron ionization had been calculated by the Keldysh – Faisal – Reiss method; the inter-electron interaction was taken into account following Ref. [58] in the Coulomb – Volkov approximation (see also Ref. [59]). This approximation is that the final state of the two electrons interacting each with other according to the Coulomb law in the presence of the external electromagnetic field is presented in the analytical form. The temporal part of the final wave function was taken as in the Volkov wave function, while the coordinate part was taken as the Coulomb wave function of the continuum spectrum. It was found in Ref. [57] that the results of such a calculation are in agreement with the experimental observation of a 'knee' in the dependence of the ion yield on the laser intensity. The simultaneous detachment of two electrons dominates at intensities less than 10^{15} W cm^2. The cascade ionization process is realized at higher intensities.

A lot of experimental and theoretical papers have been devoted to this problem over recent years [60 – 65]. However, we cannot at present give any definitive explanation for the excitation curves of some multicharged ions in the region of relatively low laser intensities.

6.4 Electron energy spectra

The electron energy spectra produced in the atomic ionization were measured in Refs [2, 18, 25, 66 – 68]. As said above, the measured electron energies far from the points where these electrons were produced, are equal to the energies immediately after the ionization process if there is no ponderomotive acceleration of the electrons by the spatial-inhomogeneous field of laser radiation. This is correct for small electron energies, short laser pulses and large focusing volumes. Then an electron is not shifted over the whole laser pulse, i.e. its energy does not change. In the opposite case the effect of ponderomotive acceleration is important; it may be taken into account if the spatial-temporal distribution of the laser intensity is known sufficiently well.

We consider here the experimental data of papers [18, 25]. They were obtained for an adiabaticity parameter $\gamma \sim 0.01$ and for a field strength less than the critical value of (5).

The duration of laser pulse in the experiment of Ref. [18] was 2.5 ps. The electrons are shifted over a distance of the order of 25 μm or less during this time, while the focusing radius is 170 μm. Hence, we can neglect the ponderomotive acceleration of electrons. The measured electron energy spectrum is shown in Fig. 9. It is in a good agreement with the experimental data of the theoretical curve calculated according to Eqn (10) for a linearly polarized field. Most of the electrons are ejected with low kinetic energies. The yield of high-energy electrons decreases exponentially.

The energy spectra for the ionization of K and Xe atoms by a long laser pulse (2 ps) were measured in Ref. [25]. The

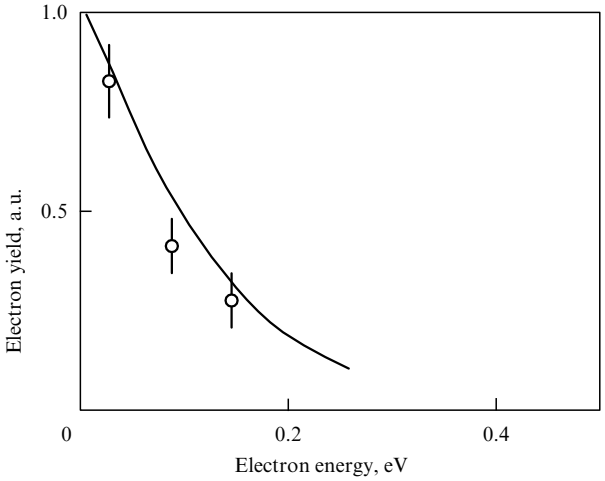

Figure 9. Electron energy spectrum in the ionization of Xe atoms by a short pulse of linearly polarized laser radiation with frequency 0.133 eV and intensity 5×10^{13} W cm^{-2} according to experimental data [18]. The theoretical curve corresponds to Eqn (10).

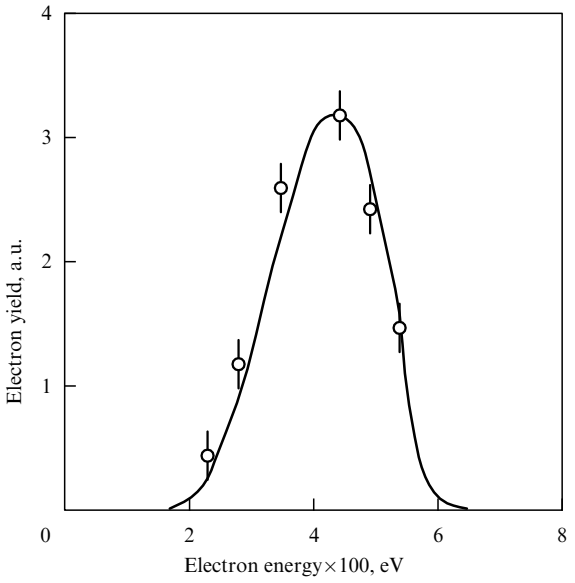

Figure 10. Electron energy spectrum for the ionization of Xe atoms by a long pulse of linearly polarized CO_2-laser radiation according to the experimental and theoretical data of Ref. [25].

ponderomotive acceleration of electrons is taken into account in the calculations, and the initial energy distribution is described by Eqn (10). The experimental and theoretical energy spectra are shown in Fig. 10. A good agreement is seen between the theory and experiment. In the case of Xe atoms the experimental data are in better agreement with theoretical predictions if the Stark shift of the energy of the ground state of an atom is taken into account (see also the calculations in Refs [13, 14]). Further, the experimental data for the ionization of singly-charged Xe ions are also in a good agreement with calculations according to Eqn (10).

The electron energy spectrum for tunneling ionization by a field of circular polarization was measured in Ref. [66]. It is shown in Fig. 11. It is seen that this energy spectrum differs strongly from the above discussed spectrum for linearly

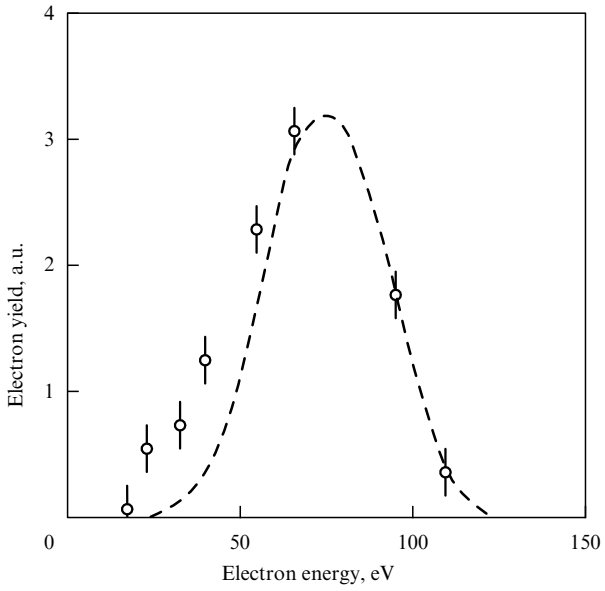

Figure 11. Electron energy spectrum for the ionization of He atoms by a short pulse of circularly polarized laser radiation with an intensity of 6×10^{15} W cm^{-2} according to the experimental data of Ref. [66]. The dotted line is the result of calculation [66] based on Eqn (19).

polarized radiation. The peak of the spectrum occurs at the energy $F^2/2\omega^2$ which is the oscillation energy of an electron in a circularly polarized field. This is in agreement with the theoretical spectrum, Eqn (19).

Thus, the observed electron energy spectra for the tunneling ionization ($\gamma < 1$, $F < F_{\mathrm{BSI}}$) agree well with the theoretical predictions.

6.5 Barrier-suppression ionization

The ionization of atoms and ions of noble gases by a laser pulse with a duration of about 1 ps and for an adiabaticity parameter $\gamma < 1$ was observed in Refs [49, 69 – 71]. The authors of these works interpreted their results as barrier-suppression ionization, since the radiation field strength exceeded the estimate (5).

However, it follows from the calculations of Ref. [72] that this conclusion is incorrect. Firstly, according to the quantum mechanical calculations of Ref. [37] for the ground state of a hydrogen atom the value of the critical field is 0.20 a.u. instead of 0.067 a.u. according to Eqn (5). Therefore the values of Eqn (5) correspond to the tunneling regime of ionization. Secondly, we should take into account the negative Stark shift of the ground atomic state. This effect also increases the critical field strength compared to estimate (5). Finally, the tunneling ionization at the edge of the laser pulse may dominate in comparison with the barrier-suppression ionization at the peak of the pulse (see also calculations of Ref. [73]).

The estimates of Ref. [72] on the assumption of a Gaussian form laser pulse show that if the duration of the laser pulse is less than 300 fs for the ionization of the ground states of noble gas atoms and less than 100 fs for the ionization of atomic ions, we can neglect tunneling ionization at the edge of laser pulse. However, the durations of the pulses in Refs [49, 69 – 71] were much larger than these. Thus, in fact, tunneling ionization at the edge of laser pulse was observed in these experiments.

Let us consider now what should be the optimal experimental conditions for the observation of above-barrier decay. It follows from the results of the calculations in Ref. [72] that an attempt to observe above-barrier decay requires strong restrictions on the parameters of the laser radiation. In the case of ionization of a Kr atom the pulse length should be less than 30 fs, and the intensity at the peak of the pulse should be greater than 3×10^{14} W cm^{-2}. In the case of multicharged ions, the requirements for the pulse length are more gentle, but for the pulse intensity are harder. So, in the case of above-barrier decay of Xe^{7+} ion the laser pulse should have a duration less than 200 fs and a peak intensity greater than 10^{16} W cm^{-2}.

Another, more realistic possibility for observing above-barrier decay is to use alkali atoms. The low ionization potentials of such atoms produce a low critical field strength (5), low ionization rates and large times for saturation in a critical field. It should be noted that the polarizability of alkali atoms is more than 10 times greater than the polarizability of noble gas atoms. However, the Stark shift of the ground states is relatively small because of the low critical fields. It follows from the calculations of Ref. [72] that the pulses should have a duration less than 1 ps and a peak intensity greater than 10^{12} W cm^{-2}. The radiation of a CO_2-laser with a large wavelength should be used in order to fulfil the condition of tunneling ionization $\gamma \ll 1$ in this case.

The above-barrier decay of atoms can be also observed under the condition $\gamma > 1$. However, for a fixed radiation field strength the conditions for pulse duration become harder with rising laser frequency, i.e. with rising adiabaticity parameter, since the saturation time in the critical field diminishes with increasing γ.

We have discussed above the conditions for the realization of above-barrier decay. Now we consider the problem of how to separate tunneling ionization and above-barrier decay in a direct experiment. It should be noted that the electron energy spectra in tunneling ionization and in above-barrier decay at $\gamma \ll 1$ are practically the same [20]. It follows from the predictions of the calculations in Ref. [21] and from the results of the experiment in Ref. [50] that the ratio of tunneling ionization rates for circular and linear polarization (at the same radiation intensity) is less than unity, and this quantity rises with radiation intensity. It is of the order of unity at the critical and greater field strengths. In the latter case it does not depend on the intensity according to the results of Ref. [20]. If in any experiment this ratio were of the order of unity, then ionization would take place in a field with above-barrier field strength.

7. Relativistic effects

In the previous sections we considered tunneling and barrier-suppression ionization in the framework of non-relativistic quantum mechanics. Thus, we assumed that the electron's velocity is small compared to the speed of light both in the initial binding state and in the final continuum state. Even for ions with multiplicity of order 10, the initial motion of the binding electron can be considered non-relativistic. However, in a strong field of laser radiation the ejected electron can obtain a relativistic energy in the final continuum state., i.e. a quantity of the order of the rest electron energy mc^2. The typical kinetic energy of an electron in a circularly polarized field is of the order of its oscillation energy $F^2/2\omega^2$. We find that relativistic effects are important for the radiation of a

CO_2-laser at a field strength higher than 6×10^9 V cm^{-1}, i.e. at an intensity higher than 5×10^{16} W cm^{-2}. If we consider visible radiation, then the required minimum value of the laser intensity rises to 5×10^{18} W cm^{-2}. Hence, above cited expressions for the ionization rates, energy and angular distributions of the ejected electrons should be generalized to the relativistic case, though above estimates are higher than in realistic experiments. We will see below that relativistic effects take place in weaker laser fields having linear polarization. Though most of the electrons are ejected with small, non-relativistic energies, we will be interested in the ejection of a small number of 'hot' electrons where relativistic effects are important.

We do not consider high-frequency fields with the laser intensities higher than in the cases of tunneling, or barrier-suppression ionization. We will see below that relativistic effects are most important in the energy and angular distributions of photoelectrons. Besides this, we will see that tunneling ionization is realized for relativistic electrons in fields that produce barrier-suppression ionization for non-relativistic electrons.

7.1. Ionization rates

The tunneling ionization rate is given by the Landau–Dykhne expression [3] (with exponential accuracy):

$$w_{\mathrm{if}} \propto \exp\left[-2\,\mathrm{Im}\int_0^{t_0}\left(E_{\mathrm{f}}(t)+E_{\mathrm{i}}\right)\mathrm{d}t\right]. \tag{49}$$

Here E_{i} is the unperturbed energy of the initial binding state, and $E_{\mathrm{f}}(t)$ is the energy of the final continuum state taking into account the field of laser radiation. The classical turning point in the complex plane of time is determined from the condition $E_{\mathrm{f}}(t_0) = -E_{\mathrm{i}}$

Let us underline that Eqn (49) is also valid in the relativistic case. Indeed, the classical action $S = P_i\,\mathrm{d}x^i$ is the relativistic invariant. The coordinate part of the classical action determines the pre-exponential factor in the transition probability only. We neglect this part in this consideration. Thus, Eqn (49) is valid in the relativistic case, and we should use the relativistic expression for the energy of the final continuum state E_{f}. In the calculations of this section we also neglect the Coulomb correction produced by the potential of the atomic core.

The adiabaticity parameter $\gamma < 1$ determines the tunneling ionization process as in the general relativistic case. Indeed, only the relativistic electron mass increases, but it is equal to its rest mass in order of magnitude.

This problem was considered in Refs [74, 75] using the approximation that relativistic effects are small, and the magneto-dipole interaction between an electron and the electric field should be taken into account in addition to the non-relativistic dipole electric interaction. The general relativistic case was considered in Ref. [76]; it operates with simple analytic expressions for the classical relativistic motion of a charged particle in the field of an electromagnetic wave.

7.2 Relativistic energy spectrum of photoelectrons

We apply the above described approach for the derivation of the relativistic energy distribution of photoelectrons in the field of *linearly* polarized low frequency laser radiation [77]. We restrict ourselves to the case of the ejection of an electron along the polarization axis of the radiation only, since most of electrons are ejected in this direction. Then the classical relativistic energy of an electron in the laser field is given by the well-known expression [78]:

$$E_{\mathrm{f}}(t) = \frac{1}{2}\sqrt{p_0^2c^2+c^4} - c^2 + \frac{p^2c^2+c^4}{2\sqrt{p_0^2c^2+c^4}}\,. \tag{50}$$

Here we put the electron's mass equal to unity, $p = p(t)$ is the electron momentum for the moment t, and $p_0 = p(0)$ is the initial electron momentum for the moment $t = 0$. The value of p is determined from the cubic equation [77]:

$$2F\frac{\sin\omega t}{\omega} = \left(1+\frac{c^4}{p_0^2c^2+c^4}\right)(p-p_0) + \frac{c^2}{3(p_0^2c^2+c^4)}\left(p^3-p_0^3\right). \tag{51}$$

Substituting Eqn (50) into (49) and taking into account Eqn (51), we obtain the relativistic energy distribution of electrons in the tunneling ionization of an atom (with exponential accuracy). We restrict ourselves to the case of moderate values of kinetic energies of ejected photoelectrons:

$$E_{\mathrm{e}} = \sqrt{p_0^2c^2+c^4} - c^2 < c^2\,,$$

i.e. to the case when this energy is less than the electron's rest energy. Then the calculation of the integral in Eqn (49) is essentially simplified, and we find

$$w_{\mathrm{if}} = w_0 \exp\left[-\frac{2E_{\mathrm{e}}\gamma^3}{3\omega} - \frac{E_{\mathrm{e}}^2\gamma}{c^2\omega}\right]. \tag{52}$$

Here the quantity w_0 is the non-relativistic ionization probability. Together with the first factor in the exponent it determines the non-relativistic energy distribution of photoelectrons in a linearly polarized field [see Eqn (10)].

It follows from Eqn (52) that the relativistic effect presented by the second term in the exponent is important under the condition $E_{\mathrm{e}} > \gamma^2c^2$. This condition does not contradict the above cited condition $E_{\mathrm{e}} < c^2$ if the adiabaticity parameter γ is small compared to unity in the tunneling regime.

Thus, the relativistic width of the energy distribution is given by

$$\Delta E_{\mathrm{e}}^{\mathrm{rel}} = c\sqrt{\frac{\omega}{\gamma}}. \tag{53}$$

For example, at $\gamma = 0.1$ the conditions $c^2 > E_{\mathrm{e}} > \gamma^2c^2$ are fulfilled in the range of kinetic energies of photoelectrons 5 keV $< E_{\mathrm{e}} <$ 500 keV. According to Eqn (53) the width of the energy distribution is of the order of 20 keV in the case of radiation of a CO_2-laser.

Thus, the conclusion can be drawn that the linearly polarized radiation of a CO_2-laser with an intensity higher than 10^{15} W cm^{-2} produces a relativistic distribution for the ejected photoelectrons with energies of the order of several keV along the polarization axis of the laser radiation, though the kinetic energies of these electrons are less than their rest mass. The results can be used for the analysis of experimental data [68].

7.3 Relativistic barrier-suppression ionization

Here we consider the relativistic approach for barrier-suppression ionization following Ref. [79]. The transition amplitude from the initial binding state to the final continuum state is given in the general relativistic case by the element of the S-matrix [80]:

$$A_{\mathrm{if}} = -\mathrm{i}\int \mathrm{d}^4x \left\langle \Psi_{\mathrm{f}}^{(V)} | A_\mu \gamma^\mu | \Psi_{\mathrm{i}}^{(0)} \right\rangle . \qquad (54)$$

Here the quantity A_μ is the relativistic 4-vector of the potential of the electromagnetic field, and γ^μ is the Dirac matrix. The wave function of the final continuum state is the relativistic Volkov wave function which satisfies the Dirac equation for an electron in the field of an electromagnetic wave.

Of course, expression (54) describes both the case of tunneling and barrier-suppression ionization. However, it does not take into account the Coulomb correction for the final wave function, so that results are valid only to exponential accuracy. Relativistic effects are important when the electron's velocity F/ω is of order of the speed of light.

Numerical calculations have been made for circularly polarized field, since in the case of linear polarization analogous calculations would be much more cumbersome. The ionization of the ground hydrogen state is considered in Ref. [79].

The most interesting results have been obtained for the angular distribution of photoelectrons. We have said above that most non-relativistic electrons are ejected in the polarization plane of circularly polarized laser radiation. However, in the relativistic case this maximum is shifted to the direction of propagation of the electromagnetic wave. The angle corresponding to the new maximum is

$$\psi_{\mathrm{d}} = \arctan\left(\frac{F}{2c\omega}\right).$$

From the physical point of view, this shift is explained by magnetic part of Lorentz force which is directed along the wave vector of the electromagnetic radiation. This effect also takes place in the case of linearly polarized radiation [74]. Thus, we can conclude that the angular distribution of photoelectrons in the case of a circularly polarized field is very sensitive to relativistic effects.

The relativistic spectrum of photoelectrons produced by circularly polarized field has a maximum at the relativistic oscillation energy of an electron. The width of this maximum increases with the electron's velocity.

8. Conclusions

The first conclusion from the results is that the condition of tunneling ionization for the adiabaticity parameter, $\gamma^2 < 1$, is also applicable for atoms and positive ions, if the radiation field strength is much less than the critical strength (5). Experimental data on ion yields are in a good agreement with the predictions of the tunneling formulae of the ADK-approach [12]. The energy spectra of photoelectrons for tunneling ionization by linearly and circularly polarized fields are also described well by simple theoretical expressions. However, in most experiments, experimenters observe tunneling ionization at the leading edge of the laser pulse, instead of barrier-suppression ionization. It is possible that only in one experiment [81] the ionization occurred in the above-barrier regime: in this work the highly-excited states of a hydrogen atom with the principal quantum numbers $n = 24 - 32$ were irradiated by a linearly polarized microwave field. The experimental data were compared to the predictions of tunneling theories. It was found that the ADK-expressions give larger values for the ionization rates compared to the experimental data. One of the possible reasons for this contradiction is that above-barrier decay occurs in this case, instead of tunneling ionization.

In conclusion it should be noted that tunneling ionization of atoms and atomic ions has been investigated in detail both experimentally and theoretically. Simple ADK-expressions well describe the experimental excitation curves for tunneling ionization. The electron energy spectra for tunneling ionization by both a linearly and circularly polarized field have been explained. However, some problems arise, for example, the so called 'knee' in the region of weak intensities on the excitation curves. Oppositely, the observation of the above-barrier decay of atoms is now only in the initial stage of investigations, since hard conditions on the parameters of radiation should be fulfilled for its realization.

This work was supported in part by the RFBR (No. 96-02-18299) and by a NATO grant. We acknowledge fruitful discussions with S L Chin.

References

1. Keldysh L V *Zh. Eksp. Teor. Fiz.* **47** 1945 (1964) [*Sov. Phys. JETP* **20** 1307 (1965)]
2. Mevel E et al. *Phys. Rev. Lett.* **70** 406 (1993)
3. Delone N B, Krainov V P *Atoms in Strong Light Fields* (Springer Series in Chemical Physics, Vol. 28) (Berlin, New York: Springer-Verlag, 1985)
4. Faisal F H M *Theory of Multiphoton Processes* (New York: Plenum Press, 1987)
5. Delone N B, Krainov V P *Multiphoton Processes in Atoms* (Berlin, New York: Springer-Verlag, 1994)
6. Chin S L, Yergeau F, Lavigne P *J. Phys. B* **18** L213 (1985)
7. Ilkov F A et al. *J. Phys. B* **25** 4005 (1992)
8. Krainov V P, Xiong W, Chin S L *Laser Phys.* **2** 467 (1992)
9. Delone N B, Kiyan I Yu, Krainov V P *Laser Phys.* **3** 312 (1993)
10. Krainov V P *J. Nonlinear Opt. Phys. Mater.* **4** 775 (1995)
11. Perelomov A M, Popov V S *Zh. Eksp. Teor. Fiz.* **50** 1393 (1966) [*Sov. Phys. JETP* **23** 924 (1966)]
12. Ammosov M V, Delone N B, Kraĭnov V P *Zh. Eksp. Teor. Fiz.* **91** 2008 (1986) [*Sov. Phys. JETP* **64** 1191 (1986)]
13. Kulyagin R V, Taranukhin V D *Laser Phys.* **3** 644 (1993)
14. Kulyagin R V, Taranukhin V D *Izv. Ross. Akad. Nauk, Ser. Fiz.* **58** (6) 161 (1994) [*Bull. Russ. Acad. Sci., Phys.* **58** 1051 (1994)]
15. Themelis S I, Nicolaides C A *Phys. Rev. A* **49** 3089 (1994)
16. Delone N B et al. *Usp. Fiz. Nauk* **131** 617 (1980) [*Sov. Phys. Usp.* **23** 472 (1980)]
17. Kraĭnov V P, Todirashku S S *Zh. Eksp. Teor. Fiz.* **83** 1310 (1982) [*Sov. Phys. JETP* **56** 751 (1982)]
18. Corkum P B, Burnett N H, Brunel F *Phys. Rev. Lett.* **62** 1259 (1989)
19. Delone N B, Krainov V P *J. Opt. Soc. Am. B* **8** 1207 (1991)
20. Krainov V P *J. Opt. Soc. Am. B* **14** 425 (1997)
21. Reiss H R *Phys. Rev. A* **22** 1786 (1980)
22. Krainov V P, Mulyukov Z S *Laser Phys.* **4** 509 (1994)
23. Goreslavsky S P, Narozhny N B, Yakovlev V P *J. Opt. Soc. Am. B* **6** 1752 (1989)
24. Kraĭnov V P, Ristic V M *Zh. Eksp. Teor. Fiz.* **101** 1479 (1992) [*Sov. Phys. JETP* **74** 789 (1992)]
25. Xiong W, Chin S L *Zh. Eksp. Teor. Fiz.* **99** 481 (1991) [*Sov. Phys. JETP* **72** 268 (1991)]
26. Kuchiev M Yu *Pis'ma Zh. Eksp. Teor. Fiz.* **45** 319 (1987) [*JETP Lett.* **45** 404 (1987)]

27. Van Linden van den Heuvell, Muller H.G., in *Multiphoton Processes* (Cambridge: Cambridge University Press, 1988)
28. Gallagher T F *Phys. Rev. Lett.* **61** 2304 (1988)
29. Muller H G *Comments At. Mol. Phys.* **24** 355 (1990)
30. Corkum P B *Phys. Rev. Lett.* **71** 1994 (1993)
31. L'Huillier A et al. *Phys. Rev. A* **48** R3433 (1993)
32. Moreno P et al. *Phys. Rev. A* **51** 4746 (1995)
33. Paulus G G et al. *J. Phys. B* **27** L703 (1994)
34. Lohr A et al. *Phys. Rev. A* **55** R4003 (1997)
35. Kraĭnov V P, Shokri B *Zh. Eksp. Teor. Fiz.* **107** 1180 (1995) [*JETP* **80** 657 (1995)]
36. Lichtenberg A J, Lieberman M A *Regular and Stochastic Motion* (Applied Mathematical Sciences, Vol. 38) (Berlin, New York: Springer-Verlag, 1983)
37. Mur V D, Popov V S *Laser Phys.* **3** 462 (1993)
38. Goreslavskiĭ S P *Zh. Eksp. Teor. Fiz.* **108** 456 (1995) [*JETP* **81** 245 (1995)]
39. Walker B et al. *Phys. Rev. Lett.* **73** 1227 (1994)
40. Lompre L A et al. *Phys. Rev. Lett.* **36** 949 (1976)
41. Boreham B W, Hughes J L *Zh. Eksp. Teor. Fiz.* **80** 496 (1981) [*Sov. Phys. JETP* **53** 252 (1981)]
42. L'Huillier A et al. *J. Phys. B* **16** 1363 (1983)
43. Chin S L, Farkas G, Yergeau F *J. Phys. B* **16** L223 (1983)
44. Walsh T D G et al. *J. Phys. B* **27** 3767 (1994)
45. Kondo K et al. *Phys. Rev. A* **48** R2531 (1993)
46. Di Mauro L F, in *Super-Intense Laser–Atom Physics* IV (Eds H G Muller, M V Fedorov) (Dordrecht: Kluwer, 1996) p. 97
47. Kondo K et al. *Phys. Rev. A* **49** 3881 (1994)
48. Augst S, Meyerhofer D D *Laser Phys.* **4** 1155 (1994)
49. Augst S et al. *J. Opt. Soc. Am. B* **8** 858 (1991)
50. Ammosov M V et al. *Laser Phys.* **7** 706 (1997)
51. Peatross J, Buerke B, Meyerhofer D D *Phys. Rev. A* **47** 1517 (1993)
52. Fittinghoff D N et al. *Phys. Rev. Lett.* **69** 2642 (1992)
53. Walker B et al. *Phys. Rev. A* **48** R894 (1993)
54. Fittinghoff D N et al. *Phys. Rev. A* **49** 2174 (1994)
55. Gibson G N et al., post-deadline report PD-1 of *Conf. on Application of High Field and Short Wavelength Sources* VII (Santa Fe, NM, March 19–22, 1997) (unpublished)
56. Landau L D, Lifshitz E M *Quantum Mechanics: Non-Relativistic Theory* 3rd edn. (Oxford, New York: Pergamon Press, 1977)
57. Golovinski P A *Laser Phys.* **7** 655 (1997)
58. Faisal F H M *Phys. Lett. A* **187** 180 (1994)
59. Becker A, Faisal F H M *Phys. Rev. A* **50** 3256 (1994)
60. Augst S et al. *Phys. Rev. A* **52** R917 (1995)
61. Kuchiev M Yu *Phys. Lett. A* **212** 77 (1996)
62. Reiss H R *Phys. Rev. A* **54** R1765 (1996)
63. Geltman S *Phys. Rev. A* **54** 2489 (1996)
64. Dietrich P et al. *Phys. Rev. A* **50** R3585 (1994)
65. Watson J B et al., in *Multiphoton Processes 1996* (Institute of Physics Conference Series, No 154, Eds P Lambropoulos, H Walther) (Bristol; Philadelphia: Institute of Physics Pub., 1997) p. 132
66. Mohideen U et al. *Phys. Rev. Lett.* **71** 509 (1993)
67. Watanabe S et al. *Phys. Rev. Lett.* **73** 2692 (1994)
68. Buerke B et al., in *Application of High Field and Short Wavelength Sources VII, OSA Technical Digest Series* **7** 75 (1997)
69. Augst S et al. *Phys. Rev. Lett.* **63** 2212 (1989)
70. Gibson G, Luk T S, Rhodes C K *Phys. Rev. A* **41** 5049 (1990)
71. Auguste T et al. *J. Phys. B* **25** 4181 (1992)
72. Ammosov M V, Delone N B *Laser Phys.* **7** 79 (1997)
73. Kiyan I Yu, Kraĭnov V P *Zh. Eksp. Teor. Fiz.* **100** 776 (1991) [*Sov. Phys. JETP* **73** 429 (1991)]
74. Krainov V P, Roshchupkin S P *Laser Phys.* **2** 299 (1992)
75. Krainov V P, Roshupkin S P *J. Opt. Soc. Am. B* **9** 1231 (1992)
76. Krainov V P, Shokri B *Laser Phys.* **5** 793 (1995)
77. Krainov V P *Opt. Express* **2** 732 (1998)
78. Landau L D, Lifshitz E M *Teoriya Polya* (The Classical Theory of Fields) 3rd edn (Oxford, New York: Pergamon Press, 1975)
79. Crawford D P, Reiss H R *Phys. Rev. A* **50** 1844 (1994)
80. Reiss H R *Prog. Quantum Electron.* **16** 1 (1992)
81. Sauer B E et al. *Phys. Rev. Lett.* **68** 468 (1992)